Biogeosciences Discuss., 9, 18479–18518, 2012
www.biogeosciences-discuss.net/9/18479/2012/
doi:10.5194/bgd-9-18479-2012

Biogeosciences Discussions

Abiotic ammonification and gross ammonium photoproduction in the upwelling system off central Chile (36° S)

A. Rain-Franco[1], C. Muñoz[1], and C. Fernandez[1,2]

[1]Departamento de Oceanografía and Centro de Investigación Oceanográfica en el Pacífico Suroriental (COPAS) Universidad de Concepción, Casilla 160–C, Concepción, Chile
[2]UPMC Univ. Paris 06 and CNRS, UMR7621, LOMIC, Observatoire Océanologique de Banyuls sur Mer, 66651, Banyuls/Mer, France

Received: 22 November 2012 – Accepted: 25 November 2012
– Published: 18 December 2012

Correspondence to: A. Rain-Franco (angelrain@udec.cl)

Published by Copernicus Publications on behalf of the European Geosciences Union.

Abstract

We investigated the production of ammonium via photodegradation of dissolved organic matter (DOM) in the coastal upwelling system off central Chile (36° S). Photoammonification experiments were carried out using exudates obtained from representative diatom species (*Chaetoceros muelleri* and *Thalassiosira minuscule*) and natural marine DOM under simulated solar radiation conditions. Additionally, we evaluated the use of photoproduced ammonium by natural microbial communities and separated ammonium oxidizing archaea and bacteria by using GC-7 as an inhibitor of the archaeal community. We found photoammonification operating at two levels: via the transformation of DOM by UV radiation (abiotic ammonification) and via the simultaneous occurrence of abiotic phototransformation and biological remineralization of DOM into NH_4^+ (referred as gross photoproduction of NH_4^+). The maximum rates of abiotic ammonification reached 0.057 µmol L^{-1} h^{-1}, whereas maximum rates of gross photoproduction reached 0.746 µmol L^{-1} h^{-1}. Our results also suggest that ammonium oxidizing archaea could dominate the biotic remineralization induced by photodegradation of organic matter and consequently play an important role in the local N cycle. Abiotic ammonium photoproduction in coastal upwelling systems could support between 7 and 50 % of the spring-summer phytoplankton NH_4^+ demand. Surprisingly, gross ammonium photoproduction (remineralization induced by abiotic ammonification) might support 50 to 180 % of spring-summer phytoplankton NH_4^+ assimilation.

1 Introduction

Since the discovery of decreasing concentrations of stratospheric ozone over the Antarctic, high levels of incident harmful solar ultraviolet radiation (specifically UV-B) have been a constant feature over the southern hemisphere, mainly during spring. The size of the ozone hole reached a historical maximum in 2006 (NASA, 2009) while unprecedented low levels were also reported over the arctic (Manney et al., 2011). In mid

BGD
9, 18479–18518, 2012

latitudes, ozone concentrations are currently 6 % lower than the long term average for the area (WMO, 2011).

The impact of the different solar spectra in the ocean can lead to deleterious effects on plankton communities (Whitehead et al., 2000; Helbling et al., 2001; Hernandez et al., 2006; Hader et al., 2007; Godoy et al., 2012). However, it is also possible to detect "positive" effects of exposure to solar radiation. For instance, the photo-dissociation of dissolved organic matter (DOM) may increase the bioavailability of dissolved organic carbon (DOC) for bacterial growth, potentially stimulating carbon transfer towards higher trophic levels via the microbial loop (Lange et al., 2003; Abboudi et al., 2007; Pakulski et al., 2007). Previous studies on the photochemical production of organic and inorganic compounds of low molecular weight via exposure of DOM to UV radiation (UVR) showed the importance of this mechanism for marine microbial activity (Bushaw et al., 1996; Mopper and Kieber, 2002; Lange et al., 2003; Kitidis et al., 2006). It is now known that the effect of UV radiation on DOM can generate among other compounds carbon monoxide (Gao and Zeep, 1998), ammonium (NH_4^+) (Bushaw et al., 1996), aminoacids (such as glutamine and alanine), nitrite (NO_2^-) and urea (Bushaw et al., 1996; Berman et al., 1999; Kieber et al., 1999; Wang et al., 2000; Mopper and Kieber, 2002; Buffam and McGlathery, 2003). Bushaw et al. (1996) demonstrated that ultraviolet radiation could increase by 20 % the availability of dissolved inorganic nitrogen (DIN) via ammonium production in rivers in the southeastern continental shelf of the United States. Wang et al. (2000) estimated that photochemically produced ammonium (photoammonification) in river waters represented up to 20 % of total organic nitrogen (TON). Additionally, other studies estimated that the photoproduction of ammonium can represent 50 % of the phytoplankton demand on the Orinoco River (Morrel and Corredor, 2001) while meeting 12 % of the estimated annual phytoplankton demand (in terms of new N) in the oligotrophic Eastern Mediterranean Sea (Kitidis et al., 2006). Therefore the potential contribution of photoammonification could vary significantly among marine biomes (Bertilsson et al., 1999; Koopmas and Bronk, 2002).

BGD
9, 18479–18518, 2012

The upwelling-system off central Chile (36° S; 73° W) in the Humboldt Current System (HCS) is one of the most productive areas of the world ocean (Daneri et al., 2000). This biological production is supported both by the assimilation of new nitrogen (as NO_3^-) (Dugdale and Goering, 1967) which is injected into the euphotic zone by mixing and vertical advection during seasonal upwelling events and regenerated nitrogen derived from in situ remineralization of organic matter (resulting in NH_4^+ release; Dugdale and Goering, 1967; Fernandez et al., 2009). Additionally, ammonium assimilation by phytoplankton is persistent throughout both upwelling and non-upwelling periods (Fernandez and Farias, 2012), representing almost half of nitrate uptake in active upwelling conditions. Recurrently high concentrations of ammonium off central Chile are also thought to be responsible for intense chemosynthetic activity via nitrification (Farias et al., 2009), particularly within the euphotic zone and oxycline (Fernandez and Farias, 2012).

The aim of this study was to evaluate the effect of solar radiation (PAR and UV) on the production of ammonium in surface waters off central Chile (36° S) in the HCS. Additionally, we evaluated the utilization of the photochemically produced ammonium by bacterioplankton in this upwelling system.

2 Methods

2.1 Study area

During this study we focused on two sites located off central Chile (36° S). First, we carried out atmospheric measurements of incident solar radiation in the Concepción area. Estimations of the depth of solar penetration in the water column were carried out via underwater measurements at Coliumo Bay off the upwelling system of central Chile (36° 49.669′ S, 73° 02.162′ W; Fig. 1).

BGD
9, 18479–18518, 2012

Due to ship availability, seawater for photoammonification experiments was collected from station 18 of the COPAS Time Series (Fig. 1). However, schedule restrictions prevented the use of radiometers for incident solar radiation profiling at st 18.

2.2 Incident solar radiation measurements

We carried out atmospheric measurements of incident radiation twice per month at noon between April 2011 and February 2012 using a portable radiometer (RM–21 Grobell ®, Germany) equipped with sensors for three spectral ranges: UV-B (defined hereafter as 280–320 nm), UV-A (defined hereafter as 320–400 nm) and PAR (defined hereafter as 400–700 nm). Values of PAR, UV-A and UV-B radiation are expressed in Wm^{-2} while integrated incident radiation will be expressed in Wm^{-1}.

The penetration of solar radiation in the water column was estimated by measuring each spectrum at two depths: 0 m (immediately below the surface) and at 0.3 m depth. Measurements were done under calm weather and low wind conditions. The coefficient of vertical light attenuation (Kd in m^{-1}) for all spectra was estimated according to Eq. (1):

$$\mathrm{Ed}(z) = \mathrm{Ed}(0) \cdot \exp(f - Kd \cdot \mathrm{Z}) \quad (1)$$

where $\mathrm{Ed}_{(Z)}$ is the irradiance at depth z and $\mathrm{Ed}_{(0)}$ is the irradiance just below the surface of the water column (Tedetti and Sempére, 2006).

The depth of 1 % penetration of incident surface irradiance ($Z_{1\%}$) was calculated for all wavelength spectra (PAR, UV-A and UV-B).

Integrated values of PAR, UV-A and UV-B were calculated by numerically integrating (trapezoidal method) radiation values between the surface and $Z_{1\%}$.

BGD
9, 18479–18518, 2012

2.3 Experiments of ammonium photo-production

2.3.1 Photo-production of ammonium from Diatom-derived DOM

We performed four experiments between September 2011 and January 2012 in order to evaluate the production of ammonium via photo-transformation of labile DOM derived from representative diatom cultures (Table 1).

DOM was obtained from cultures of two species present of the study area: *Chaetoceros muelleri* (Lemmermann, 1898) and *Thalassiosira minuscule* (Krasske, 1841). Cultures were maintained in Walne+Si media and filtered through precombusted 0.7 µm filters (Millipore^{TM}; 450 °C for 6 h) in order to obtain exudates, which were irradiated with either full solar radiation (PAR+UV) or UV radiation (UV-A+UV-B) for 2 and 4 h respectively. Samples submitted to PAR+UV and UV radiation only were incubated in 500 mL quartz bottles. Doses received by all treatments are reported in Table 1. Dark control samples were incubated in darkened 500 mL Duran Schott bottles. Additionally, poisoned controls (amended with 1000 µL of 6 % $HgCl_2$) were made for each treatment in order to avoid microbial ammonium remineralization. All experiments were performed using an irradiation chamber (UV Chamber B–03, Gröbel ®, Germany) equipped with either PAR+UV or UV-A and UV-B lamps. This instrument is equipped with an internal temperature control system that allowed having low temperature variations during the experiments.

2.3.2 Photo-production of ammonium from marine DOM

Another set of experiments was designed to evaluate the production of ammonium from marine DOM using natural seawater samples. Seawater (25 L) was taken at 5 m depth at the COPAS time series st 18 (R/V *Kay Kay II*, Table 2 and Fig. 1). During each sampling, a CTD cast was done (SeaBird) in order to determine the structure of the water column. Additionally, chlorophyll *a* concentrations were determined by fluorometry at University of Concepción.

BGD
9, 18479–18518, 2012

Experiments were carried out during spring (November 2011). Water samples were filtered through precombusted GF/F 0.7 µm filters (450 °C, 6 h) using a peristaltic pump. Filtrates were distributed in autoclaved 500 mL glass bottles (Duran Schott for dark control) or 500 mL quartz bottles (UV-A+UV-B treatment). The time of exposure to UV radiation was 4 h followed by 2 h of incubation in dark conditions.

Samples for ammonium (in triplicate) and bacterioplankton abundance were taken before incubation and every 2 h. For ammonium determination, 20 mL samples were amended with 5 mL of Phthaldialdehyde for fluorometry (OPA) and stored in the dark at room temperature until analysis by the fluorometric method using a Turner Design fluorometer (Holmes et al., 1999). Determination of nitrite (NO_2^-) and nitrate (NO_3^-) was made in duplicate in 10 mL samples, which were frozen until laboratory analysis using a colorimetric automatic technique (Bran Luebbe ® autoanalyzer) following Aminot and Kérouel (2007). Bacterioplankton abundance was determined by flow cytometry according to Marie et al. (2000). Samples (1350 µL) were taken in duplicate in sterile cryovials, amended with glutaraldehyde (at 0.1 % final concentration) and stored at −80 °C until laboratory analysis at PROFC laboratory at University of Concepcion.

2.3.3 Response of ammonium oxidizing microorganisms to photo-produced ammonium

The response of bacterioplankton to in situ photoproduced ammonium was evaluated using surface seawater (5 m depth, 25 L) coming from COPAS st 18. Experiments were carried out in September 2011 and January 2012 (austral spring and summer). Samples were filtered through precombusted GF/F 0.7 µm filters (450 °C, 6 h) with a peristaltic pump. Because of previously reported ammonium oxidizing archaeal activity in the area (Belmar et al., 2011), we assessed bacterial and archaeal activity separately by amending one set of samples with N1-guanyl-1, 7-diaminoheptane (GC–7), an inhibitor of archaeal-activity (Jansson et al., 2000; Levipan et al., 2007; Fernandez and Farias, 2012). Samples were then distributed in three treatments: exposure to PAR+UV radiation in quarts bottles (500 mL), exposure to PAR radiation (full light conditions

BGD
9, 18479–18518, 2012

using 500 mL glass Duran Schott bottles) and dark conditions (darkened 500 mL glass Duran Schott bottles). Incubations lasted 4 h without dark incubation time.

Samples for nitrate, nitrite, ammonium and bacterioplankton abundance were taken and analyzed as described in the previous section.

2.4 Quantifying ammonium photo-production

In order to accurately estimate ammonium photoproduction we took into consideration the presence of bacterioplankton in samples filtered through 0.7 µm and therefore assumed that in situ regeneration of ammonium can occur during the incubation. Samples incubated in dark conditions allowed estimating dark ammonium regeneration while our poison controls allowed checking background ammonium levels during the incubation and the occurrence of abiotic ammonification. Consequently, in order to correctly estimate ammonium photoproduction we established the following assumptions: (1) the exposure of DOM samples to UV radiation or PAR+UV radiation always results in ammonium production (other labile N compounds are not taken into account) (2) photolysis of DOM only occurred under exposure to UV radiation and was absent in dark controls or PAR exposed samples (3) complete degradation of DOM leading to limitation does not occur during the experiments (4) bacterial ammonium regeneration is constant during the incubation. Based on these assumptions we propose Eq. (2) for estimating the ammonium production by photolysis of the DOM.

Equation (2) evaluates the change in the ammonium concentration through exposure to UV radiation, while taking into account the simultaneous ammonium production that takes place via remineralization of DOM by bacterioplankton activity or ammonium consumption.

$$\left[\underset{\text{Total}}{\overset{+}{\underset{4}{\text{NH}}}}\right]\left(\mu\text{mol}\,\text{L}^{-1}\right) = \left(\left[\underset{\text{T1}}{\overset{+}{\underset{4}{\text{NH}}}}\right] - \left[\underset{\text{T0}}{\overset{+}{\underset{4}{\text{NH}}}}\right]\right)_{\text{Exposure}} - \left(\frac{\left(\left[\text{NH}_4^+\right]_{\text{T1}} - \left[\text{NH}_4^+\right]_{\text{T0}}\right)}{\text{n}^\circ\,\text{cel}_{\text{T1}}}\right)_{\text{Dark}} * \left(\text{n}^\circ\,\text{cel}_{\text{T1}}\right)_{\text{Exposure}} \quad (2)$$

BGD
9, 18479–18518, 2012

The term $[NH_4^+]_{T0}$ represents the ammonium concentration at the beginning of the incubation. The term $[NH_4^+]_{T1}$ represents the ammonium concentration at the end of the incubation. The term $[NH_4^+]_{Total}$ represents total ammonium production via photolysis. The term $n^\circ cell_{T1}$ represents the bacterioplankton abundance measured at the end of the incubation. The sub-indexes "Exposure" and "Dark" identify exposed samples from the dark controls.

2.5 Data analysis

Data of ammonium concentration during photoproduction experiments were analyzed by a paired t-test. Ammonium, nitrite, nitrate concentrations and bacterioplankton abundances of ammonium utilization experiments were analyzed by a one-way ANOVA (Analysis of Variance) after checking for normality assumption (Kolmogorov-Smirnov test, $\alpha = 0.05$) and homoscedasticity (Cochran test, $\alpha = 0.05$). Finally, pairwise multiple comparison were performed using the Tukey test as an *a posteriori* test ($\alpha = 0.05$).

3 Results

3.1 Incident solar radiation in the study area

The mean value per month of incident atmospheric PAR (700–400 nm), UV-A (400–320 nm) and UV-B (320–280 nm) radiation measured in the Concepcion area (36° S) is shown in Fig. 2a. Data for all spectra followed the expected seasonal trend with lower values occurring during autumn and winter months (April to August 2011) compared to spring and summer (September 2011 to February 2012). The lowest values for PAR, UV-A and UV-B radiation were found in June ($77.18 \pm 53.08\,Wm^{-2}$, $8.00 \pm 4.55\,Wm^{-2}$ and $0.21 \pm 0.12\,Wm^{-2}$, respectively) while the maximum values of the study period were found in December 2011 ($346.78 \pm 50.19\,Wm^{-2}$, $35.23 \pm 4.09\,Wm^{-2}$ and $1.61 \pm 0.22\,Wm^{-2}$ for PAR, UV-A and UV-B, respectively). The intensity of UV-A was

BGD
9, 18479–18518, 2012

always higher than UV-B (up to 37 times higher). Mean intensity values of UV-A radiation in winter 2011 were $12.3 \pm 4.1\,Wm^{-2}$, while in summer 2012 it reached $30.3 \pm 5.3\,Wm^{-2}$. UV-B radiation on the other hand showed a mean winter value for 2011 of $0.35 \pm 0.14\,Wm^{-2}$, while in the summer 2012 it increased to $1.42 \pm 0.19\,Wm^{-2}$.

The penetration of solar radiation in the water column (as $Z_{1\%}$) at Coliumo Bay is shown in Fig. 2b and 2. As expected, the monthly mean value of $Z_{1\%}$ during the entire study period was higher for PAR radiation than for UV-A and UV-B (9.4 m vs. 4.4 m and 3.2 m, respectively). For PAR, the maximum penetration was found in winter 2011 (29.7 m in May). Minimum penetration values were observed in summer and reached 2.9 m in December 2011. UV-A radiation also penetrated at a maximum depth of 7.4 m in winter (May 2011) and only 1.6 m in summer (December 2011). This was also the case for UV-B radiation, for which maximum penetration was found in spring (November 2011) with 5.1 m and summer (3.1 ± 1.2 m) and the minimum was found in May (1.5 m).

Integrated solar radiation in the water column for PAR, UV-A and UV-B spectra is reported in Fig. 2c. Values varied significantly during the study period with PAR showing maximum values in winter (max. $581.49\,Wm^{-1}$ in May 2011 Fig. 2a) while for UV-A radiation the maximum value was found in late spring (November 2011, $41.748\,Wm^{-1}$; Fig. 2b) and corresponds to a penetration level of 7.1 m within the period of highest incident radiation ($33.74 \pm 4.43\,Wm^{-2}$; Fig. 2a). Finally, the integrated intensity of UV-B was lower than for PAR and UV-A reached a maximum value at the end of spring (November, $1.21\,Wm^{-1}$) which coincides with a period of intense incident UV-B radiation ($1.36 \pm 0.26\,Wm^{-2}$; Fig. 3a) and the highest penetration (5.1 m).

3.2 Photoproduction of ammonium from diatom-derived DOM

Experiments were designed in order to evaluate the photoproduction of ammonium from exudates of two representative phytoplankton species, *C. muelleri* and *T. minuscule*.

BGD
9, 18479–18518, 2012

Ammonium production was detected in all samples of *C. muelleri* (Fig. 3a) although it was significantly higher in samples exposed to PAR+UV (t-test, $P = 0.012$ and $P = 0.001$, respectively) compared to dark samples. Rates of abiotic NH_4^+ production reached 0.008 µmol L^{-1} h^{-1} in poisoned samples exposed to UV radiation. This production can be associated to the abiotic generation of ammonium via DOM photodegradation. Ammonium production in non-poisoned exposed samples on the other hand can be attributed to biological activity as well as DOM photodegradation and exceeded by 17 times the rates of abiotic ammonium production obtained in the poisoned control. Ammonium was produced in non-poisoned dark samples, presumably by microbial remineralization only and reached 0.013 µmol L^{-1} h^{-1}. The estimated ammonium photo-production (removing dark remineralization according to Eq. 2) reached 0.128 µmol L^{-1} h^{-1}.

The variation of ammonium concentrations in exudates of *C.muelleri* exposed to PAR+UV radiation versus dark conditions is shown in the Fig. 3b. Higher ammonium concentrations were detected in samples exposed to solar radiation compared to the dark condition (t-test paired, $P = 0.0399$). Nevertheless ammonium concentrations decreased during the incubation at a rate of 0.002 µ mol L^{-1} h^{-1} and 0.100 µmol L^{-1} h^{-1} for light-exposed and dark samples respectively (i.e. a 50 fold difference between both treatments). Nevertheless ammonium photoproduction could be estimated according to Eq. (2) as 0.096 µmol L^{-1} h^{-1}.

Ammonium production in exudates of *C. muelleri* exposed only to UV radiation is shown in Fig. 3c. Concentrations were generally higher in the treatment exposed to UV radiation than in the dark control (t-test paired, $P = 0.020$). Ammonium levels increased during the incubation in samples exposed to UVR at a rate of 0.616 µmol L^{-1} h^{-1}, while decreasing in the dark control at a rate of 0.076 µmol L^{-1} h^{-1}. The estimated rates of ammonium photo-production according to Eq. (2) reached 0.746 µmol L^{-1} h^{-1}.

Exposure of exudates of *T. minuscule* to UV radiation lead to ammonium production in the poisoned as well as non-poisoned samples (t-test $P = 0.0024$ and $P < 0.001$, respectively; Fig. 4a). Abiotic ammonium production in poisoned samples reached

BGD
9, 18479–18518, 2012

$0.057\,\mu mol\,L^{-1}\,h^{-1}$ while in non poisoned samples values were higher and reached $0.654\,\mu mol\,L^{-1}\,h^{-1}$. Ammonium production in both treatments exceeded rates observed in the dark control ($0.374\,\mu mol\,L^{-1}\,h^{-1}$; Fig. 4a). Estimated ammonium photoproduction according to Eq. (2) reached a rate of $0.28\,\mu mol\,L^{-1}\,h^{-1}$.

The variation of ammonium concentrations during exposure of *T. minuscule* exudates to PAR+UV radiation is shown in the Fig. 4b. In this experiment, higher ammonium concentrations were found in the exposed samples compared to dark conditions (paired t-test, $P = 0.0253$). The observed ammonium production rate reached $0.056\,\mu mol\,L^{-1}\,h^{-1}$ in the exposed treatment while in the dark control ammonium was consumed at a rate of $0.011\,\mu mol\,L^{-1}\,h^{-1}$. Estimated ammonium photo-production was $0.088\,\mu mol\,L^{-1}\,h^{-1}$. This value is lower than the estimated rate obtained for exudates of *C.muelleri* exposed to the same radiation regime ($0.096\,\mu mol\,L^{-1}\,h^{-1}$). Ammonium production was also observed in exudates of *T. minuscule* exposed only to UV radiation as shown in the Fig. 4c. Ammonium concentrations were higher in the treatment exposed to light compared to dark conditions (paired t-test, $P = 0.0242$). The rate of ammonium production was $0.494\,\mu mol\,L^{-1}\,h^{-1}$ which is higher than the rate obtained for the dark samples ($0.146\,\mu mol\,L^{-1}\,h^{-1}$). Therefore, estimated ammonium photo-production was of $0.356\,\mu mol\,L^{-1}\,h^{-1}$.

3.3 Photoproduction of ammonium in natural samples and response of microbial assemblages to insitu ammonification.

Hydrographic conditions during sampling for the three natural DOM photodegradation experiments (September, November 2011 and January 2012) are shown in Fig. 5a and b. During September 2011 (early spring), temperature varied between 12.6 in surface waters and 9.47 °C in near bottom layers. The thermocline was located at 20 m depth while the MLD and $Z_{1\%}$ were approximately located at 10 m depth. Total chlorophyll-concentrations reached $17.18\,mg\,m^{-3}$ in near surface waters and rapidly decreased to near 0 values at 30 m depth (Fig. 5a). Conditions during November 2011 (spring)

BGD
9, 18479–18518, 2012

showed higher SST values (13.65 °C) and a shallow thermocline (10 m). Temperature in near bottom waters was close to 9.78 °C (Fig. 5b). Total chlorophyll-*a* concentrations showed a subsurface maximum (17.795 mg m^{-3}) at 5 m and a rapid decrease at 20 m depth. The MLD was only 10 m deep while the euphotic zone $Z_{1\%}$) reached 35 m depth. During January 2012 (summer), temperature varied from 16.38 to 10.65 °C along the water column, with a strong termocline around 15 m (Fig. 5c). Total chlorophyll-*a* concentrations were lowest that in autumn and spring with maximum concentration in surface waters (6.04 mg m^{-3}) and near 0 values at 20 m depth. The depth of MLD was 10 m while the euphotic zone ($Z_{1\%}$) reached 15 m (Fig. 5c).

Ambient ammonium concentrations (Fig. 5) were higher in November 2011 compared to September 2011 and January 2012. During September 2011 (Fig. 5a) there were two subsurface maximum concentrations at 20 and 80 m (0.33 and 0.97 µmol L^{-1}, respectively) while surface values reached (0.11 µmol L^{-1}). In November 2011 (Fig. 5b), ambient ammonium in surface waters was higher compared to early spring and reached (0.22 µmol L^{-1}). Subsurface concentrations were also high and reached 3.05 µmol L^{-1} at 20 m depth while near bottom waters values were close to 1.1 µmol L^{-1}. During January 2012 (Fig. 5c) surface ammonium concentration was close to 0.04 µmol L^{-1} and increased to 1.463 µmol L^{-1} at 10 m depth. Ammonium then decreased with depth until 50 m (0.022 µmol L^{-1}), and increased again in near bottom waters (0.741 µmol L^{-1}).

We evaluated ammonium production via photodegradation of marine DOM by UV radiation (UV-A+UV-B). The results of this experiment (November 2011) are shown in Fig. 6. Ammonium concentrations decreased during the first 2 h of exposure at a rate of 0.047 µmol L^{-1} h^{-1} and reached concentrations of 4.783 ± 0.063 µmol L^{-1} (Fig. 6a). After 4 h of exposure, concentrations reached values close to 4.23 ± 0.33 µmol L^{-1}. Incubation in dark conditions (2 h) resulted in lowest NH_4^+ concentrations in the sample (3.761 ± 0.022 µmol L^{-1}). Ammonium concentrations in dark samples decreased during the first 2 h of exposure but increased towards the end of the exposure period (4.535 ± 0.195 µmol L^{-1} after 2 h and 6.330 ± 0.230 µmol L^{-1}

BGD
9, 18479–18518, 2012

after 4 h). Finally, ammonium concentrations during dark incubations decreased to $4.408 \pm 0.190\ \mu mol\ L^{-1}$. Even if no significant difference was obtained between the treatment exposed to UV and the dark control (paired t-test, $P = 0.1145$), we estimated ammonium photo-production for the first 2h of exposure at a rate of $0.047\ \mu mol\ L^{-1}\ h^{-1}$.

Nitrite concentrations (Fig. 6b) were significantly higher in the samples exposed to UV radiation compared to the dark control (t-test paired, $P = 0.0303$). After 4 h of exposure, concentrations increased in both treatments ($0.500 \pm 0.132\ \mu mol\ L^{-1}$ and $0.280 \pm 0.057\ \mu mol\ L^{-1}$ for exposed and dark control, respectively) with respect to initial levels ($0.241 \pm 0.009\ \mu mol\ L^{-1}$). Dark conditions resulted in higher nitrite concentrations in both treatments, although values in the exposed samples exceeded those found in the dark control ($1.317 \pm 0.496\ \mu mol\ L^{-1}$ and $0.627 \pm 0.024\ \mu mol\ L^{-1}$ final concentrations respectively).

Nitrate concentrations (Fig. 6c) increased after 4 h of UV exposure, and were higher in exposed samples compared to dark conditions ($2.41 \pm 0.98\ \mu mol\ L^{-1}$ and $1.64 \pm 0.26\ \mu mol\ L^{-1}$, respectively). Nitrate levels continued to increase in dark conditions in both treatments and reached $7.57 \pm 1.84\ \mu mol\ L^{-1}$ in the exposed samples while the dark control showed lower values ($4.41 \pm 0.87\ \mu mol\ L^{-1}$). However, differences were not significant between both treatments (t-test paired, $P = 0.0573$).

Interestingly, bacterioplankton abundance (Fig. 6d) was significantly lower in samples exposed to UVR compared to samples incubated in the dark (paired t-test, $P = 0.002$). Cell abundance after 2 h of exposure to UVR decreased in the exposed samples ($186 \pm 6 \times 10^3\ cell\ mL^{-1}$), whereas dark samples showed no change compared to initial values ($313 \pm 12 \times 10^3\ cell\ mL^{-1}$). After 4 h of exposure, cell abundance increased in the dark control while decreasing in the treatment exposed to UV radiation ($337 \pm 7 \times 10^3\ cell\ mL^{-1}$ and $172 \pm 10 \times 10^3\ cell\ mL^{-1}$). During dark incubations, the abundance of bacterioplankton also decreased in the treatment exposed to UV, reaching lower values than the dark control ($153 \pm 0 \times 10^3\ cell\ mL^{-1}$ and $356 \pm 7 \times 10^3\ cell\ mL^{-1}$).

BGD
9, 18479–18518, 2012

The in situ utilization of photo-produced ammonium by natural marine microbial communities is reported in Fig. 7. Samples retrieved in early spring (September 2011) were exposed to PAR radiation only, full solar radiation (PAR+UV) and dark conditions during 4 h (Fig. 7a). An archaea-specific inhibitor (GC-7; Jansson et al., 2000; Levipan et al., 2007; Fernandez and Farias, 2012) was applied to duplicate samples (Fig. 7b). After 4 h of incubation, ammonium concentrations increased in the samples exposed to PAR+UV radiation ($3.35 \pm 0.411\ \mu mol\ L^{-1}$) compared to samples exposed to PAR radiation only ($2.19 \pm 0.121\ \mu mol\ L^{-1}$; Tukey test, $P < 0.05$). Dark controls on the other hand did not show significant differences in ammonium concentrations compared to PAR and PAR+UV treatments (Tukey test, $P > 0.05$). This suggests an effect of PAR and/or UV radiation in ammonium production. Following Eq. (2), we estimated the rate of photoproduction of ammonium in the treatment exposed to PAR+UV radiation as $0.201\ \mu mol\ L^{-1}\ h^{-1}$.

The variations in NO_3^- and NO_2^- during the experiment are shown are the Fig. 7a and b. After 4 h of incubation, an increased in nitrate concentrations was observed in all treatments compared to T0 ($9.037 \pm 0.026\ \mu mol\ L^{-1}$). Treatment exposed to PAR+UV radiation reached the highest concentration ($9.71 \pm 0.25\ \mu mol\ L^{-1}$) while samples exposed to PAR and dark conditions showed values close to $9.48 \pm 0.01\ \mu mol\ L^{-1}$ and $9.28 \pm 0.057\ \mu mol\ L^{-1}$, respectively. Nitrite concentrations were lower than ammonium and nitrate levels. Nitrite values at T0 were of $0.517 \pm 0.009\ \mu mol\ L^{-1}$ and decreased after 4 h of incubation in samples exposed to PAR and PAR+UV radiation ($0.464 \pm 0.004\ \mu mol\ L^{-1}$ and $0.436 \pm 0.018\ \mu mol\ L^{-1}$, respectively) while remained virtually constant in the dark control ($0.515 \pm 0.003\ \mu mol\ L^{-1}$).

The evolution of bacterioplankton abundances during these experiments are shown in Fig. 7. In early spring, bacterioplankton abundances in samples exposed to PAR radiation increased from $318 \pm 16 \times 10^3\ cell\ mL^{-1}$ to $398 \pm 141 \times 10^3\ cell\ mL^{-1}$ after 4 h of incubation. On the contrary, samples exposed to PAR+UV as well as the dark control showed a decrease in cell counts over time ($316 \pm 10 \times 10^3\ cell\ mL^{-1}$ and $296 \pm 15 \times 10^3\ cell\ mL^{-1}$, respectively), although no significant difference was

BGD
9, 18479–18518, 2012

found among all treatments (ANOVA one way, $P = 0.7638$). Samples amended with GC-7 showed a significant decrease in ammonium concentrations (Tukey test, $P > 0.05$) throughout the experiment compared to initial values ($2.8 \pm 0.12\,\mu mol\,L^{-1}$; Fig. 7b). After 4 h of incubation, the dark control showed higher ammonium concentrations ($2.474 \pm 0.053\,\mu mol\,L^{-1}$) than treatments exposed to PAR and PAR+UV ($2.212 \pm 0.18\,\mu mol\,L^{-1}$ and $2.301 \pm 0.02\,\mu mol\,L^{-1}$, respectively). The lowest concentrations were found in the samples exposed to PAR radiation, probably due to the absence of ammonium photoproduction and active ammonium consumption during the incubation (at a rate of $0.036\,\mu mol\,L^{-1}\,h^{-1}$).

Nitrate concentrations also increased in all treatments with respect to initial values ($9.15 \pm 0.077\,\mu mol\,L^{-1}$). The treatment exposed to PAR+UV showed the highest average nitrate concentration ($10.175 \pm 0.127\,\mu mol\,L^{-1}$) while treatments exposed to PAR and dark control reached concentrations of $9.879 \pm 0.112\,\mu mol\,L^{-1}$ and $9.165 \pm 0.851\,\mu mol\,L^{-1}$ respectively. Initial nitrite concentrations were $0.518 \pm 0.003\,\mu mol\,L^{-1}$; after the incubation lower concentrations were observed in all treatments. Concentrations in samples exposed to PAR+UV radiation ($0.455 \pm 0.001\,\mu mol\,L^{-1}$) were lower than values obtained in samples exposed to PAR radiation only or to dark conditions ($0.463 \pm 0.004\,\mu mol\,L^{-1}$ and $0.492 \pm 0.034\,\mu mol\,L^{-1}$, respectively). Samples amended with GC-7 showed a decrease in bacterioplankton abundance in the treatments exposed to PAR ($315 \pm 13 \times 10^3\,cell\,mL^{-1}$) and PAR+UV ($309 \pm 5 \times 10^3\,cell\,mL^{-1}$). On the contrary, values increased in the dark control ($323 \pm 7 \times 10^3\,cell\,mL^{-1}$; Fig. 7b) although the observed difference among all treatments were not significant (one way ANOVA, $P = 0.4144$).

The experiments carried out in summer (January 2012; Fig. 7c) showed a stronger effect of PAR+UV on ammonium concentrations compared to samples exposed to PAR radiation only and the dark control (Tukey test, $P < 0.05$). Samples exposed to PAR+UV radiation showed a decrease in ammonium concentrations with respect to the initial concentrations ($0.939 \pm 0.047\,\mu mol\,L^{-1}$ vs. $0.747 \pm 0.003\,\mu mol\,L^{-1}$). Also, and as observed in our spring experiments described above, samples exposed to

BGD
9, 18479–18518, 2012

PAR radiation only showed the lowest ammonium concentrations during the incubation ($0.580 \pm 0.025\,\mu mol\,L^{-1}$). The estimated rate of ammonium photoproduction for samples exposed to UV radiation reached $0.057\,\mu mol\,L^{-1}\,h^{-1}$.

Nitrate and nitrite variation in this experiment is shown in Fig. 7c and d. Nitrate concentrations decreased in all treatments during the incubation ($0.166 \pm 0.086\,\mu mol\,L^{-1}$). Interestingly, samples exposed to PAR as well as dark controls showed nitrate concentrations below the detection limit, while in samples exposed to PAR+UV nitrate concentrations reached $0.112 \pm 0.0\,\mu mol\,L^{-1}$ at the end of the incubation period. Nitrite concentrations in the treatment exposed to PAR radiation, varied from $0.053 \pm 0.01\,\mu mol\,L^{-1}$ at T0 to $0.046 \pm 0.003\,\mu mol\,L^{-1}$ at the end of the incubation. Samples exposed to PAR+UV on the other hand showed an increase in concentrations and reached $0.055 \pm 0.011\,\mu mol\,L^{-1}$. As seen for nitrate, nitrite concentrations in the dark control were below the detection limit. Bacterioplankton abundances in these experiments (Fig. 7c and d) showed an increase in bacterioplankton abundances in the treatment exposed to PAR radiation only ($15132 \pm 1029 \times 10^3\,cell\,mL^{-1}$ vs. $13930 \pm 457 \times 10^3\,cell\,mL^{-1}$). In contrast, samples exposed to PAR+UV as well as the dark control showed decreasing abundances after 4 h of incubation (12632 ± 0 and $11367 \pm 2240 \times 10^3\,cell\,mL^{-1}$, respectively). In spite of the observed differences, results between treatments were not significantly different between each other (one way ANOVA, $P = 0.1583$). When GC-7 was added to the samples, as inhibitor of archaeal activity, results showed generally lower ammonium concentrations compared to non-amended samples (Fig. 7a and c), and also decreasing concentrations during the incubation. Final values after 4 h of incubation were nonetheless significantly higher (Tukey test, $P < 0.05$) in the treatment exposed to PAR and PAR+UV ($0.483 \pm 0.009\,\mu mol\,L^{-1}$ and $0.473 \pm 0.002\,\mu mol\,L^{-1}$) than in the dark controls ($0.382 \pm 0.007\,\mu mol\,L^{-1}$). In this case the estimated rate of ammonium photo-production reached $0.02\,\mu mol\,L^{-1}\,h^{-1}$.

The initial concentrations of nitrate were close to $0.166 \pm 0.086\,\mu mol\,L^{-1}$ and decreased during the experiment to values below the detection limit for samples exposed to PAR and PAR+UV. In the dark control on the other hand, concentrations

BGD
9, 18479–18518, 2012

also decreased but were close to $0.03 \pm 0.000\,\mu mol\,L^{-1}$ after 4 h of incubation. Nitrite concentrations increased in samples exposed to PAR+UV radiation as well as in the dark control ($0.057 \pm 0.004\,\mu mol\,L^{-1}$ and $0.059 \pm 0.006\,\mu mol\,L^{-1}$, respectively vs. $0.053 \pm 0.010\,\mu mol\,L^{-1}$), but there was not a significant difference among all treatments (one way ANOVA, $P = 0.05764$). However in the treatment exposed to PAR radiation only, concentrations decreased during incubation and reached $0.05 \pm 0.000\,\mu mol\,L^{-1}$ as a final value. Bacterioplankton abundance (Fig. 7d) decreased in samples exposed to PAR radiation (final abundance $7539 \pm 329 \times 10^3$ cell mL^{-1}). These values were lower (Tukey test, $P < 0.05$) than samples exposed to PAR+UV radiation and the dark control ($8604 \pm 70 \times 10^3$ cell mL^{-1} and $8875 \pm 135 \times 10^3$ cell mL^{-1}, respectively).

4 Discussion

4.1 Variability of solar radiation in the study area

During this study we used a portable radiometer for measuring incident PAR and UV radiation. We also evaluated the occurrence of photoammonification and the simultaneous response of marine bacterial communities.

Our incident radiation data complements previous attempts to establish a time series of PAR and UVR in central Chile (Hernandez et al., 2011). However, although available data sets are complementary they may not be entirely comparable because the known differences of the instruments used in both cases. Our average UV-A values reported for winter 2011 are lower than data reported by Hernandez et al., (2011) for previous years (2003–2004). Our average UV-B values for winter and summer were also 4 and 3 fold lower than the reported by Hernandez et al. (2011). Nonetheless, the results of measurements of solar radiation show that level increased by 2.6, 2.6 and 4.2 fold for PAR, UV-A and UV-B in winter compare to summer, respectively, following a coherent seasonal trend. A latitudinal comparison shows that UV-A (320–400 nm) values reported for lower and higher latitudes in Chile (Santiago, 33°33′ and Punta Arenas,

BGD
9, 18479–18518, 2012

53°08′; Cabrera et al., 1995) are similar while our data reports lower values of UV-B (280–320 nm) for the same latitudes.

The depth of penetration of solar radiation (as PAR, UV-A and UV-B) between May 2011 and February 2012 varied seasonally in the study area, with a decrease in values between autumn 2011 and summer 2012. Maximum penetration was observed during autumn (April and May 2011), which coincides with the end of active upwelling conditions in the study area. As a consequence, turbidity decreases in the water column allowing deeper penetration of solar radiation. Nevertheless, UV radiation (both UV-A and UV-B) was measurable in the coastal area off central Chile during the entire study period (Fig. 2), suggesting a potential year-round impact in the first meters of the water column. Values of depth penetration ($Z_{1\%}$) reached 29.7 m for PAR, 7.4 m for UV-A and 5.1 m for UV-B. Although PAR $Z_{1\%}$ seems deeper than expected for a productive upwelling system, it is coherent with time data gathered historically at st 18 (unpublished data COPAS Time Series program). Our obtained values are on the other hand lower than previous studies for open ocean waters at the same latitude (36° S; 74° W; Godoy et al., 2012) and are in the same range of estimations as $Z_{10\%}$ reported for Seno Reloncavi and Valdivia in southern Chile (Huovinen and Gomez, 2011). However, since our $Z_{1\%}$ estimations include the assumption of a homogeneous water column (Whitehead et al., 2000) and values of integrated solar radiation are affected by the intensity of incident solar radiation and the optical properties of the water column, comparing our results with existing data must be done carefully. As stated previously, the variety of instruments used for underwater measurement of UV radiation precludes safe comparisons (see review by Tedetti and Sempére, 2006).

High integrated values obtained in this study (up to 581, 25 and 1 Wm^{-1} of PAR, UV-A and UV-B respectively, Fig. 2) corresponded to the deepest values of $Z_{1\%}$ (in autumn) while in summer, when the mixed layer heat balance is dominated by solar radiation (Sobarzo et al., 2007), high integrated values responded to higher intensity of incident radiation but not deeper $Z_{1\%}$. This can be explained by the increased turbidity of the water column during the productive season which combines biological

BGD
9, 18479–18518, 2012

particles (phytoplankton and bacterioplankton) and high sedimentation rates previously observed in the study area (Montero et al., 2007).

We also report a persistent exposure of the first meters of the water column to UV-A and UV-B during the year. As it has been observed that incident solar radiation may intervene in the photoproduction of bioavailable compounds for bacterioplankton (Lange et al., 2003) or have negative effects such as DNA damage (Hebling et al., 2001), inhibition of photosynthesis (Arrigo et al., 2003; Holm-Hansen et al., 1997) and decrease of bacterioplankton production (Hernandez et al., 2006), direct measurements of the optical properties of the water column are needed to complement these results. This include the concentration and distribution of chromophoric dissolved organic matter (CDOM), which is a major contributor to the penetration of solar radiation in the ocean water (Whitehead et al., 2000).

4.2 Ammonium photoproduction from diatom cultures

Ammonium production via exposure of diatom-derived DOM to PAR+UV and UV radiation was observed in two different types of cultures: *C. muelleri* and *T. minuscule*. Because cultures were filtered through 0.7 µm we assume that some bacterial activity may occur except in poisoned samples. The exudates of *C. muelleri* and *T. minuscule* showed ammonium production by PAR+UV and UVR in non-poisoned as well as poisoned samples (Figs. 3a and 4a). Final ammonium concentrations were always higher in non-poisoned compared to poisoned samples and resulted in higher rates of ammonium production (Table 4). Rates in exposed samples were also higher than in dark controls. We concluded than abiotic ammonification occurred in poisoned samples and reached an average value of $0.033 \pm 0.03\,\mu mol\,L\,h^{-1}$. Also, we observed that PAR+UV radiation exposure resulted in enhanced ammonium production in non poisoned samples, which was higher than dark controls. These experiments carried out with exudates of representative diatom species allowed estimating the time scale of ammonium photoproduction, which can occur within 2 to 4 h of exposure (Figs. 3 and 4). Additionally,

BGD
9, 18479–18518, 2012

the samples exposed to UVR showed higher ammonium production rates than the samples exposed to PAR+UV radiation (Table 3).

4.3 Ammonium photoproduction from natural DOM samples

The production of ammonium from DOM coming from natural marine samples was not clearly detected in all experiments (Fig. 6). Ammonium concentrations were constant in samples exposed to UV for 2 h but decreased dramatically after 4 h of incubation with no recovery in dark conditions. In accordance, bacterioplankton abundance decreased during the entire experiment. On the contrary, dark samples generated high concentrations of NH_4^+, but also showed a rapid consumption during the last period of incubation that was followed by a constant increase in bacterioplankton abundance (Fig. 6d). Interestingly, simultaneously measured NO_3^- and NO_2^- showed a consistent increase in both treatments (although concentrations were higher in exposed samples) that was maintained during dark incubation time (Fig. 6b and c) indicating active ammonium oxidation activity (nitrification, although heterotrophic uptake of NH_4^+ cannot be ruled out but was not assessed in these experiments). Consequently, the lack of photoammonification in our natural samples might be explained by, among other factors, active microbial NH_4^+ utilization (specifically nitrification) during the incubation (in spite of solar radiation exposure) and high levels of DOM present in this coastal upwelling system (Montero et al., 2007) that could eventually protect microorganisms from photoinhibition (Merbt et al., 2011). The response of microbial communities to NH_4^+ produced during exposure to UVR seems to coincide with its utilization at short time scales suggesting that specific communities can resist short term exposure to full sunlight as it has been observed in laboratory cultures with nitrifying strains (Fernandez, unpublished data).

BGD
9, 18479–18518, 2012

4.4 Microbial response to photodegradation: remineralization induced by photolysis of DOM

We observed different patterns in community response to photoproduced NH_4^+ depending on the presence of archaea in the sample. Ammonium production occurred mainly when the archaeal community was present in the sample and exposed to PAR+UVR. In contrast, when the archaeal community was inhibited, we observed decreasing ammonium concentrations, possibly because ammonium consumption exceeded ammonium photoproduction in the samples exposed to PAR+UV radiation (Fig. 7b and d). These results suggest that archaeal community could mediate active biotic remineralization coupled with DOM photolysis and consequently play an important role in the gross photoproduction of ammonium in highly productive systems. However they also suggest that utilization of photoproduced ammonium (mainly as ammonium oxidation) potentially occurs irrespectively of microbial community composition (although it was successfully quantified in the presence of bacteria rather than archaea).

The exposure to PAR radiation only also showed different patterns. Total bacterioplankton abundance increased after exposure to PAR radiation (Fig. 7a). However when the archaeal community was inhibited, bacterioplankton abundance did not vary (Fig. 7b). On the other hand, ammonium concentrations showed a stronger decrease in the presence of total bacterioplankton than in the absence of archaea. A possible explanation includes active heterotrophic activity induced by PAR radiation. Our results are however not consistent with the results of Merbt et al. (2011) who found increased photosensitivity of ammonium-oxidizing archaea (AOA) compared to ammonium-oxidizing bacteria (AOB), being the AOA more sensitive to radiation of 400–680 nm than AOB. The study carried out by Chuch et al., (2010) in the Pacific Ocean on the other hand showed that in the first 100 m depth (Pacific Ocean) *amoA* genes were relative low, but contrasted with high abundance of *amoA* transcriptors. Also, they contradict previous assumptions on the sensitivity of nitrifying bacterial communities to solar radiation (Olson, 1981; Guerrero and Jones, 1996a and b). It has

BGD
9, 18479–18518, 2012

been suggested that photochemically produced nitrogen can increase the productivity of N-limited microbial assemblages in the Baltic Sea (Vähätalo and Järvinen, 2007) and also that photodegradation of organic matter can benefit photoheterotrophic bacterial communities (Vähätalo et al., 2011). Our results support these scenarios and show a potentially important role of archaea on gross ammonium photoproduction and a consistent bacterial nitrification activity fueled by DOM photodegradation under solar radiation exposure.

These findings and the general knowledge of the abundance of archaeal communities in the upper water column of the study area (Belmar et al., 2011) suggest a complex scenario for the local nitrogen cycle that needs to be further investigated in order to achieve a better understanding of the processes fueling biological production in this system.

5 Conclusions

This study reports ammonium photo-production in a coastal upwelling system and its potential contribution to the local nitrogen budget. Exposure of exudates of representative diatoms (*C.muelleri* and *T. minuscule)* and natural DOM to solar radiation showed the occurrence at short times scales (2 or 4 h) of two concomitant processes related to the photochemical remineralization of ammonium. First, abiotic ammonification via UV radiation was observed in poisoned samples, in agreement with previous studies (Table 4). In this case the exposure to sunlight (primarily UV-A radiation, Vähätalo and Järvinen, 2007) causes breakdown of dissolved organic matter (DOM) and consequent release of NH_4^+(Gao and Zeep, 1998; Gardner et al., 1998; Bushaw-Newton and Moran, 1999; Buffam and McGlathery, 2003). Our rates with diatom exudates were smaller than previously reported values (Bushaw et al., 1996; Gao and Zeep, 1998), but are in the same range of results reported by Bushaw-Newton and Moran (1999), Buffam and McGlathery (2003) and Kitidis et al., (2006) as seen in Table 4. They were

BGD
9, 18479–18518, 2012

nevertheless higher than rates obtained by Buffam and McGlathery (2003) and Kitidis et al. (2006) for oligotrophic and coastal lagoon waters.

The second mechanism seems to be related with microbial activity in the samples exposed to PAR and UV radiation. The fragmentation of DOM leading to the formation of labile compounds such as glicine and alanine (Buffam and McGlathery, 2003; Tar et al., 2001) results in its subsequent degradation by bacterioplankton and ammonium production (Berman et al., 1999; Mooper and Kieber, 2002). This remineralization induced by photolysis, contributes to the final result that tides these two processes as gross ammonium production mediated by photolysis of DOM. The coupled photochemical-biological pathway of ammonium production has been studied previously in different environments such as freshwater systems (Lindell et al., 1995) and marine costal waters (Miller and Moran, 1997). Those studies proved the importance of sequential photochemical-biological degradation of organic matter for bacterial growth (Lindell et al., 1995; Mopper and Kieber, 2002). Our results come to complement these observations by focusing on ammonium contribution. Based in existing phytoplankton N uptake data for the study area (Fernandez and Farías, 2012), we estimated that abiotic ammonification can occur after a few hours of exposure and could support between 7 and 50 % of spring-summer phytoplankton NH_4^+ demand. Surprisingly, gross ammonium photoproduction (the coupling between abiotic ammonification and remineralization induced by photodegradation of DOM) might support 50 to 180 % of spring-summer phytoplankton NH_4^+ assimilation. These values are higher than the potential contribution of photochemically produced N to phytoplankton new production in the Baltic Sea where N deprived communities directly react to bioavailable N (Vähätalo and Järvinen, 2007).

Although photoammonification has been suggested to be stronger in shelf waters and marginal seas (Kitidis et al., 2006), neither abiotic nor gross ammonium photoproduction are accounted for in regional nitrogen budgets. Our results therefore have important implications for the understanding the mechanisms sustaining primary production in coastal upwelling systems.

BGD
9, 18479–18518, 2012

Acknowledgements. This study was carried out in the frame of the International Associated Laboratory (LIA) MORFUN and FONDECYT project 1100358. Diatom cultures were kindly provided by the Laboratory of Microalgae Culture at University of Concepción. Chlorophyll-*a* data was provided by the COPAS center. We thank Hector Levipan, Claudio Iturra and the organic geochemistry (GO Lab) at UdeC for valuable help during the development of this study and manuscript. We thank Wade Jeffrey for valuable comments that greatly improved the manuscript.

References

Abboudi, M., Jeffrey, W. H., Ghiglione, J.-F., Pujo-Pay, M., Oriol, L., Sempére, R., Charriere, B., and Joux, F.: Effects of photochemical transformations of dissolved organic matter on bacterial metabolism and diversity in three contrasting coastal sites in the northwestern Mediterranean sea during summer, Microb. Ecol., 55, 344–357, 2007.

Aminot, A. and Kérouel, R.: Dosage automatique des nutriments dans les eaux marines, Editions Quae., p. 188 , 2007.

Arrigo, K., Lubin, D., Van Dijken, G., Holm-Hansen, O., and Morrow, E.: Impact of a deep ozone hole on Southern Ocean primary production, J. Geophys. Res., 108, 3154, 19 pp., doi:10.1029/2001JC001226, 2003.

Belmar, L., Molina, V., and Ulloa, O.: Abundance and phylogenetic identity of archaeoplankton in the permanent oxygen minimum zone of the eastern tropical South Pacific, FEMS Microbiol. Ecol., 78, 314–326, 2011.

Berman, T., Bechemin, C., and Maestrini, S.: Release of ammonium and urea from dissolved organic nitrogen in aquatic ecosystems, Aquat. Microb. Ecol., 16, 295–302, 1999.

Bertilsson, S., Stepanauskas, R., Cuadros-Hansson, R., Granéli, W., Wikner, J., and Travik, L.: Phochemically induced changes in bioavailable carbon and nitrogen pools in boreal watershed, Aquat. Microb. Ecol., 19, 47–56, 1999.

Buffam, I., and McGlathery, K.: Effect of ultraviolet light on dissolved transformations in coastal lagoon water, Limnol. Oceanogr., 48, 723–734, 2003.

Bushaw, K., Zeep, R., Matthew, A., Schulz-Janders, D., Bourbonniere, R., Bronk, D., and Moran, M.: Photochemical release of biologically available nitrogen from aquatic dissolved organic matter, Nature, 381, 404–407, 1996.

BGD

9, 18479–18518, 2012

Bushaw-Newton, K. and Moran, M.: Photochemical formation of biologically available nitrogen from dissolved humic substances in coastal marine systems, Aquat. Microb. Ecol., 18, 285–292, 1999.
Church, M., Wai, B., Kart, D., and DeLong, E.: Abundances of crenarchaeal amoA genes and transcrips in the Pacific Ocean, Environ. Microbiol., 12, 679–688, 2010.
Daneri, G., Dellarossa, V., Quiñones, R., Jacob, B., Montero, P., and Ulloa, O.: Primary production and community respiration in the Humbolt Current system off Chile and associated oceanic areas, Mar. Ecol.-Prog. Ser., 197, 41–49, 2000.
Dugdale, R. and Goering, J.: Uptake of new and regenerated forms of nitrogen in primary productivity, Limnol. Oceanogr., 12, 196–206, 1967.
Farías, L., Fernández, C., Faúndez, J., Cornejo, M., and Alcaman, M. E.: Chemolithoautotrophic production mediating the cycling of the greenhouse gases N_2O and CH_4 in an upwelling ecosystem, Biogeosciences, 6, 3053–3069, doi:10.5194/bg-6-3053-2009, 2009.
Farman, J., Gardiner, G., and Shanklin, J.: Large losses of total ozone in Antarctica reveal seasonal ClO_x/NO_x interaction, Nature, 315, 207–210, 1985.
Fernandez C. and Farías L.: Assimilation and regeneration of inorganic nitrogen in a coastal upwelling system: ammonium and nitrate utilization, Mar. Ecol.-Prog. Ser., 451, 1–14, 2012.
Fernandez, C., Farías, L. and Alcamán, M.: Primary production and nitrogen processes in surface waters of the Peruvian upwelling system, Progr. Oceanog., 83, 159–168, 2009.
Gao, R. and Zeep, R.: Factors influencing photoreactions of dissolved organic matter in a coastal river of the southeastern United States, Environ. Sci. Technol., 32, 2940–2946, 1998.
Gardner, W., Cavaletto, J., Bootsma, H., Lavrentyev, P. J., and Troncone, F.: Nitrogen cycling rates and light effects in tropical lake Maracaibo, Venezuela, Limnol. Oceanogr., 43, 1814–1825, 1998.
Godoy, N., Canepa, A., Lasternas, S., Mayol, E., Ruíz-Halpern, S., Agustí, S., Castilla, J. C., and Duarte, C. M.: Experimental assessment of the effect of UVB radiation on plankton community metabolism along the Southeastern Pacific off Chile, Biogeosciences, 9, 1267–1276, doi:10.5194/bg-9-1267-2012, 2012.
Guerrero, M. and Jones, R.: Photoinhibition of marine nitrifying bacteria I: wavelength response, Mar. Ecol. Prog. Ser., 141, 183–192, 1996a.
Guerrero, M. and Jones, R.: Photoinhibition of marine nitrifying bacteria II: dark recovery after monochromatic or polychromatic irradiation, Mar. Ecol. Prog. Ser., 141, 193–198, 1996b.

BGD
9, 18479–18518, 2012

Hader, D.-P., Kumar, H., Smith, R., and Worrest, R..: Effects of solar UV on aquatic ecosystems and interactions with climate change, Photoch. Photobio. Sci., 6, 267–285, 2007.
Helbling, E. W., Buma, A., Karin de Boer, M., and Villafañe, V. E.: In situ impact of solar ultraviolet radiation on photosynthesis and DNA in temperate marine phytoplankton, Mar. Ecol.-Prog. Ser., 211, 43–49, 2001.
Hernández, K., Quiñones, R., Daneri, G., and Helbling, E.W.: Effects of solar radiation on bacterioplankton production in the upwelling system off central-southern Chile, Mar. Ecol.-Prog. Ser., 315, 19–31, 2006.
Holm-Hansen, O., Villafañe, V. E., and Helbling, E. W.: Effects of solar ultraviolet radiation on primary production in Antarctic waters, in: Antarctic communities: Species, structure and survival, edited by: Battaglia, B., Valencia, J., and Walton, D. W. H., Cambridge University Press, Cambridge, 375–380, 1997.
Holmes, R., Aminot, A., Kérouel, R., Hooker, B., and Peterson, B.: A simple and precise method for measuring ammonium in marine and freshwater ecosystems, Can. J. Fish. Aquat. Sci., 56, 1801–1808, 1999.
Huovinen, P. and Gomez, I.: Spectral attenuation of solar radiation in Patagonian fjord and coastal waters and implications for algal photobiology, Cont. Shelf Res., 31, 254–259, 2011.
Jansson, B., Malandrin, L., and Johansson, H. E.: Cell cycle arrest in archaea by the hypusination inhibitor N1-guanyl-1, 7-diaminoheptane, J. Bacteriol., 182, 1158–1161, 2000.
Kieber, R., Li, A., and Seaton, P.: Production of nitrite from the photodegradation of dissolved organic matter in natural waters, Environ. Sci. Technol., 33, 993–998, 1999.
Kitidis, V., Uher, G., Upstill-Goddard, R. C., Mantoura, R. F. C., Spyres, G., and Woodward, E. M. S.: Photochemical production of ammonium in the oligotrophic Cyprus Gyre (Eastern Mediterranean), Biogeosciences, 3, 439–449, doi:10.5194/bg-3-439-2006, 2006.
Koopmans, D.J. and Bronk, D.: Photochemical production of dissolved inorganic nitrogen and primary amines from dissolved organic nitrogen in waters of two estuaries and adjacent surficial groundwaters, Aquat. Microb. Ecol., 26, 295–304, 2002.
Lange, H., Morris, D., and Williamson, C.: Solar ultraviolet photo-degradation of DOC may stimulate freshwater food webs, J. Plankton Res., 25, 111–117, 2003.
Levipan, H. A., Quiñones, R., and Urrutia, H.: A time series of prokaryote secondary production in the oxygen minimum zone of the Humboldt Current system, off central Chile, Progr. Oceanog., 75, 531–549, 2007.

BGD
9, 18479–18518, 2012

Lindell, M., Granéli, W., and Tranvik, L.: Enhanced bacterial growth in response to photochemical transformation of dissolved organic matter, Limnol. Oceanogr., 40, 195–199, 1995.
Manney, G. L., Santee, M., Rex, M., Livesey, N. J., Pitts, M. C., Veefkind, P., Nash, E. R., Wohltmann, I., Lehmann, R., Froidevaux, L., Poole, L., Schoeberl, M. R., Haffner, D. P., Davies, J., Dorokhov, V., Gernandt, H., Johnson, B., Kivi, R., Kyro, E. Larsen, N., Levelt, P. F., Makshtas, A., McElroy, C., Nakajima, H., Parrondo, M. C., Tarasick, D. W., von der Gathen, P., Walker, K. A., and Zinoviev, N. S.: Unprecedented Arctic ozone loss in 2011, Nature, 478, 469–475, 2001.
Marie, D., Simon, N., Guillou, L., Partensky, F., and Vaulot, D.: Flow cytometry analysis of marine picoplankton, in: In living color: protocols in flow cytometry and cell sorting, edited by: Diamond, R. A., and DeMaggio, S., Springer, Berlin, 421–454, 2000.
Merbt, S., Stahl, D., Casamayor, E., Marti, E., Graeme, N., and Prosser, P.: Differential photoinhibition of bacterial and archaeal ammonia oxidation, FEMS Microbiol. Lett., 327, 41–46, 2011.
Miller, L. and Moran, M.: Interaction of photochemical and microbial processes in the degradation of refractory dissolved organic matter from a coastal marine environment, Limnol. Oceanogr., 42, 1317–1324, 1997.
Montero, P., Daneri, G., Cuevas, L. A., Gonzalez, H. E., Jacob, B., Lizarraga, L., and Menschel, E.: Productivity cycles in the coastal upwelling area off Concepcion: The importance of diatoms and bacterioplankton in the organic carbon flux, Prog. Oceanog., 75, 518–530, 2007.
Mopper, K. and Kieber, D.: Photochemistry and the cycling of carbon, sulfur, nitrogen and phosphorus, in: Biochemistry of marine dissolved organic matter, edited by: Hansell, D. and Carlson, C., Academic Press, 455–489, 2002.
Morel, J. and Corredor, J.: Photomineralization of fluorescent dissolved organic matter in the Orinoco river plume: Estimation of ammonium release, J. Geophys. Res., 106, 16807–16813, 2001.
Nasa: Ozone hole watch, annual record since 1979, http///ozonewatch.gsfc.nasa.gov/index.Html,(last accaess: 03 December 2012).
Olson, R. J.: Differential photoinhibition of marine nitrifying bacteria: a possible mechanism for the formation of the primary nitrite maximum, J. Mar. Res., 39, 227–238, 1981.

BGD
9, 18479–18518, 2012

Pakulski, J. D., Baldwin, A., Dean, A. L., Durkin, S., Karentz, D., Kelley, C. A., Scott, K., Spero, H. J., Wilhelm, S. W., Amin, R., and Jeffrey, W. H.: Responses of heterotrophic bacteria to solar irradiance in the eastern Pacific Ocean, Aquat. Microb. Ecol., 47, 153–162, 2007.
Sobarzo, M., Bravo, L., Donoso, D., Garces-Vargas, J., and Schneider, W.: Coastal upwelling and seasonal cycles that influence the water column over the continental shelf off central Chile, Prog. Oceanog., 75, 363–382, 2007.
Tarr, M., Wang, W., Bianchi, T., and Engelhaupt, E.: Mechanisms of ammonia and amino acid photoproduction from aquatic humic and colloidal matter, Water Res., 35, 3688–3696, 2001.
Tedetti, M., and Sempére, R.: Penetration of ultraviolet radiation in the marine environment: A review, Photochem. Photobiol., 82, 389–397, 2006.
Vähätalo, A. and Järvinen, M.: Photochemically produced bioavailable nitrogen from biologically recalcitrant dissolved organic matter stimulates production of a nitrogen-limited microbial food web in the Baltic Sea, Limnol. Oceanogr., 52, 132–143, 2007.
Vähätalo, A., Aarnos, H., Hoikkala, L., and Lignell, R.: Photochemical transformation of terrestrial dissolved organic matter supports hetero-and autotrophic production in coastal waters, Mar. Ecol. Prog. Ser., 423, 1–14, 2011.
Wang, W., Matthew T., Bianchi, T., and Engelhaupi, E.: Ammonium protoproduction from aquatic humic and colloidal matther, Aquat. Geochem., 6, 275–292, 2000.
Whitehead R., De Mora, S., and Demers, S.: Enhanced UV radiation – a new problem for the marine environment, in: The effects of UV radiation in the marine environment, edited by: de Mora, S., Demers, S., and Vernet, M., Cambridge University Press, Cambridge, 1–34, 2000.
WMO (World Meteorological Organization), Scientific Assessment of Ozone Depletion: 2010, Global Ozone Research and Monitoring Project–Report No. 52, 516 pp., Geneva, Switzerland, 2011.

BGD
9, 18479–18518, 2012

Table 1. Summary of ammonium photoproduction experiments carried out with exudates of cultured marine diatoms.

Date	Type of sample	Cell Density (cell mL^{-1})	Range of exposure	Exposure time (h)		Dose Kj m^{-2}		
				Radiation	Dark	PAR	UVA	UVB
21-09-2011	*C. muelleri*	3.97×10^6	PAR+UV-A+ UV-B	2	0	150	203	4
11-10-2011	*C. muelleri*	2.52×10^6	PAR + UV-A + UV-B	5	0	374	507	11
	T. minuscule	2.82×10^6						
11-11-2011	*C. muelleri*	4.44×10^6	UV-A + UV-B	5	2		272	832
	T. minuscule	3.65×10^6						
21-09-2011	*T. minuscule*	3.41×10^6	UV-A + UV-B	4	0		218	665

BGD
9, 18479–18518, 2012

Table 2. Summary of ammonium photoproduction experiments with marine samples carried out during this study.

Date	Range of Exposure	Exposure time (h) Radiation	Dark	Dose (Kj m^{-2}) PAR	UV-A	UV-B
13-09-2011	PAR + UV-A + UV-B	4	0	299	406	9
21-11-2011	UV-A + UV-B	4	2		218	665
11-01-2012	PAR + UV-A + UV-B	4	0	299	406	9

BGD
9, 18479–18518, 2012

Table 3. Summary of NH_4^+ photoproduction rates obtained during this study.

Date	Type sample	Range of Exposure	Exposure Time (h)	Abiotic Ammonification ($\mu mol\,L^{-1}\,h^{-1}$)	Gross photoproduction ($\mu mol\,L^{-1}\,h^{-1}$)
21-09- 2011	Exudates				
	Chaetocerosmuelleri	PAR+UV-A+ UV-B	2	0.008	0.128
11-10-2011	Exudates				
	Chaetocerosmuelleri	PAR+UV-A+ UV-B	5		0.096
	Thalassiora minuscule	PAR+UV-A+ UV-B	5		0.088
11-11-2011	Exudates				
	Chaetocerosmuelleri	UV-A + UV-B	5		0.746
	Thalassiora minuscule	UV-A + UV-B	5		0.356
23-01-2011	Exudates				
	Thalassiora minuscule	UV-A + UV-B	4	0.057	0.28
13-09-2011	Seawater	PAR+UV-A+ UV-B	4		−0.261
22-11-2011	Seawater	UV-A + UV-B	4		0.047
11-01-2012	Seawater	PAR+UV-A+ UV-B	4		0.020–0.057

BGD
9, 18479–18518, 2012

Table 4. Rates of ammonium photoproduction obtained from the literature (in $\mu mol\,L^{-1}\,h^{-1}$) for freshwater, estuarine and marine environments.

Type of Samples	Abiotic Ammonification ($\mu mol\,L^{-1}\,h^{-1}$)	References
freshwater, estuarine isolated humics	0.05–0.37	Bushaw et al. (1996)
freshwater, estuarine isolated humics	0.1	Gao and Zeep, (1998)
Freshwater	0	Jorgensen et al. (1998)
Freshwater	0	Bertilson et al. (1999)
coastal lagoon	−0.29	Gardner et al. (1998)
Estuarine	0.007–0.06	Bushaw-Newton and Moran, (1999)
coastal lagoon	0.001–0.046	Buffam and McGlathery, (2003)
marine, filtered by 0.1 µm	0.0004–0.0029	Kitidis et al. (2006)
Exudates *Chaetoceros muelleri*		
filtered by 0.7 µm	0.096–0.746	this study
filtered by 0.7 µm, with mercury chloride	0.008	this study
Exudates *Thalassiosira minuscule*		
filtered by 0.7 µm	0.088–0.356	this study
filtered by 0.7 µm, with mercury chloride	0.057	this study
marine coastal waters	0.057–0.204	this study

BGD
9, 18479–18518, 2012

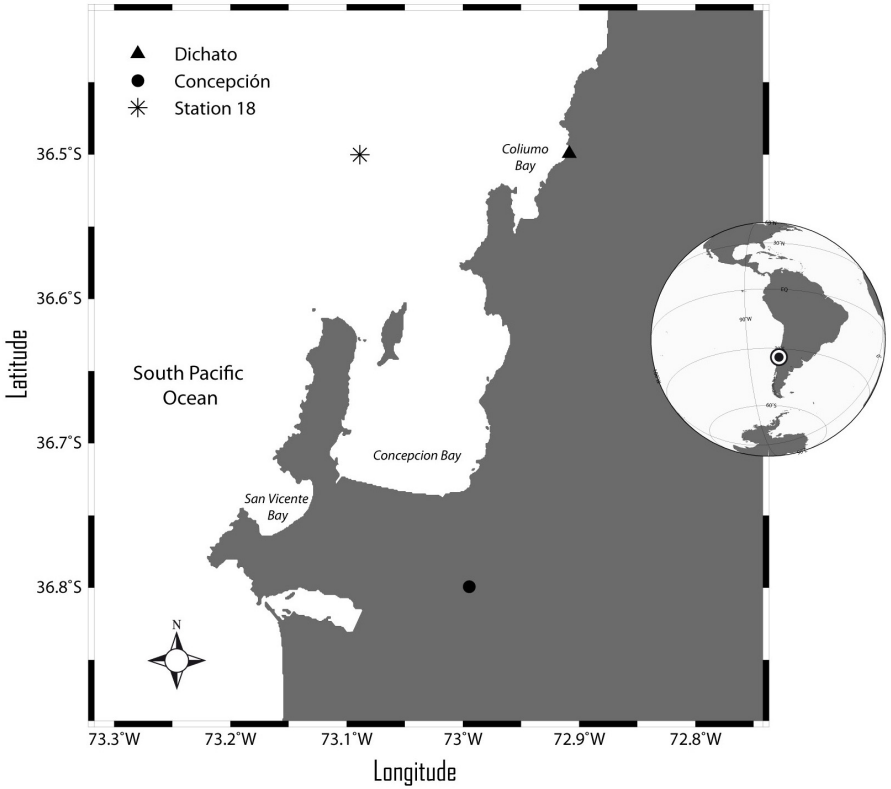

Fig. 1. Location of the study area and sampling sites for ammonium photoproduction experiments (COPAS Time Series st 18*), incident irradiance (Concepción •) and measurements of light penetration in the water column (Coliumo Bay ▲).

BGD
9, 18479–18518, 2012

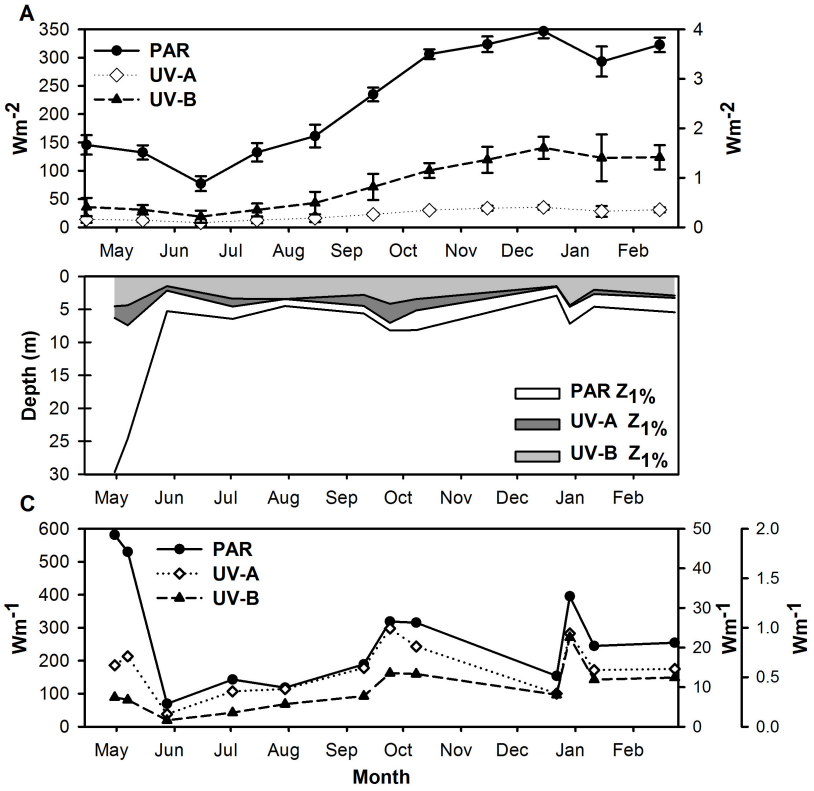

Fig. 2. (A) Time Series of average values of incident UVR measured at noon in the Concepción area, central Chile (April and February 2012). **(B)** Depth penetration ($Z_{1\%}$) of solar radiation at noon between May 2011 and February 2012 in the coastal area of central Chile. **(C)** Time Series of the intensity of incident radiation integrated between the surface and the depth of 1 % irradiance penetration of PAR (left axis), UV-A (right axis) and UV-B (secondary right axis).

BGD
9, 18479–18518, 2012

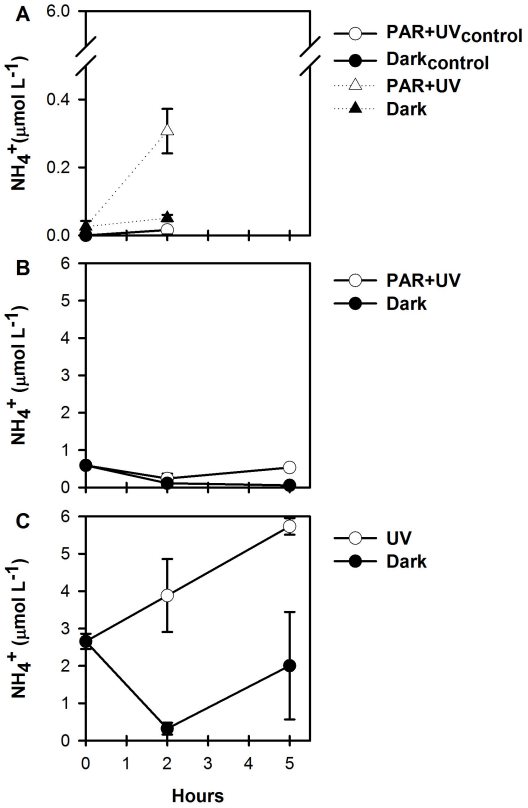

Fig. 3. DOM photodegradation experiments using exudates from *C.muelleri*. Ammonium concentrations during exposure to **(A)** PAR + UVR compared to poisoned and dark control samples **(B)** PAR + UVR compared to dark control samples **(C)** UVR compared to dark control samples.

BGD
9, 18479–18518, 2012

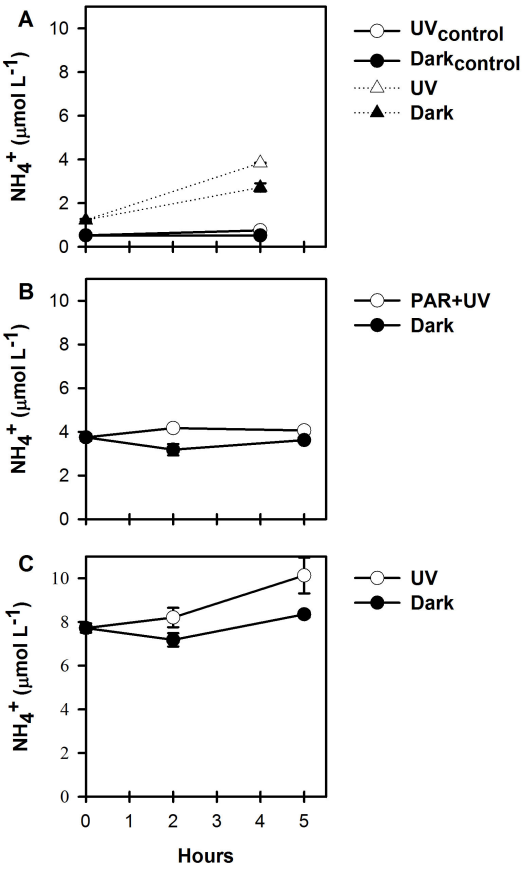

Fig. 4. Evolution of ammonium concentrations during experiments of dissolved organic matter photodegradation using exudates of cultured *T. minuscule*. **(A)** Exposure to UV radiation compared to dark and poisoned controls. **(B)** Exposure to PAR + UVR in poisoned samples and dark control and **(C)** exposure to UVR compared to dark controls.

BGD
9, 18479–18518, 2012

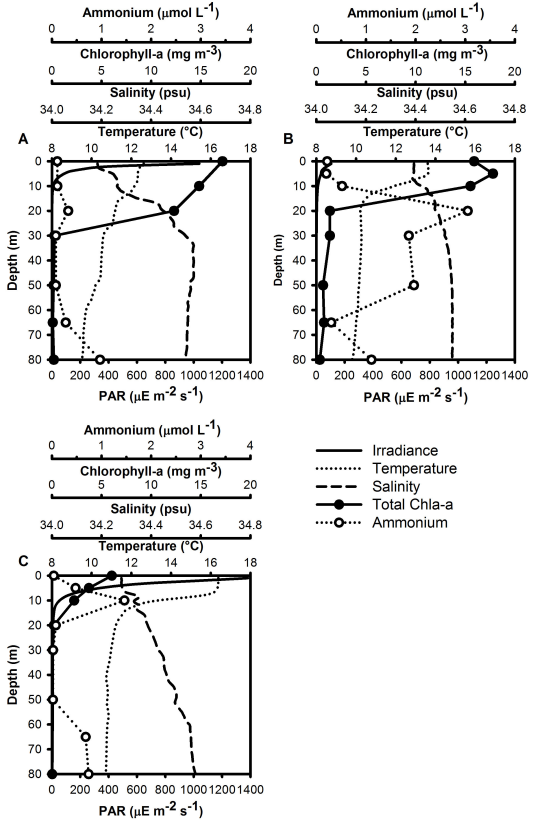

Fig. 5. Hydrographic conditions (CTD profiles) of irradiance, salinity, temperature and ambient concentrations of total chlorophyll-a and ammonium for the experiments carried out in **(A)** September 2011, **(B)** November 2011 and **(C)** January 2012.

BGD
9, 18479–18518, 2012

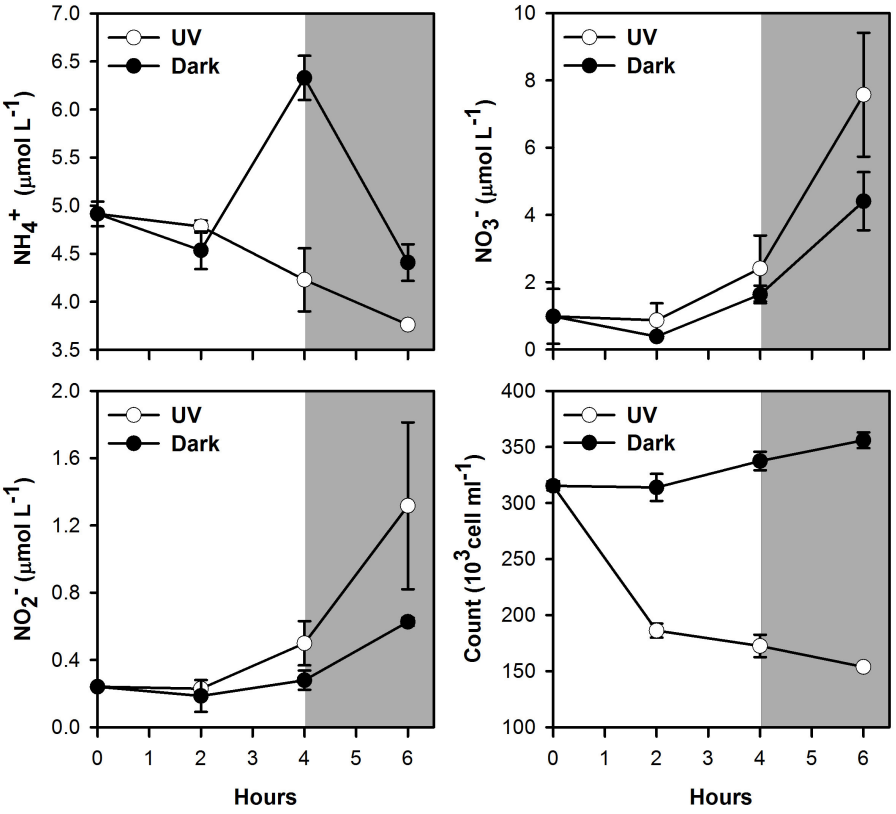

Fig. 6. Ammonium **(A)**, nitrite **(B)** and nitrate **(C)** concentrations and bacterioplankton abundance **(D)** during DOM photodegradation experiments using marine samples exposed to UVR (white area) followed by a dark incubation period (grey area).

BGD
9, 18479–18518, 2012

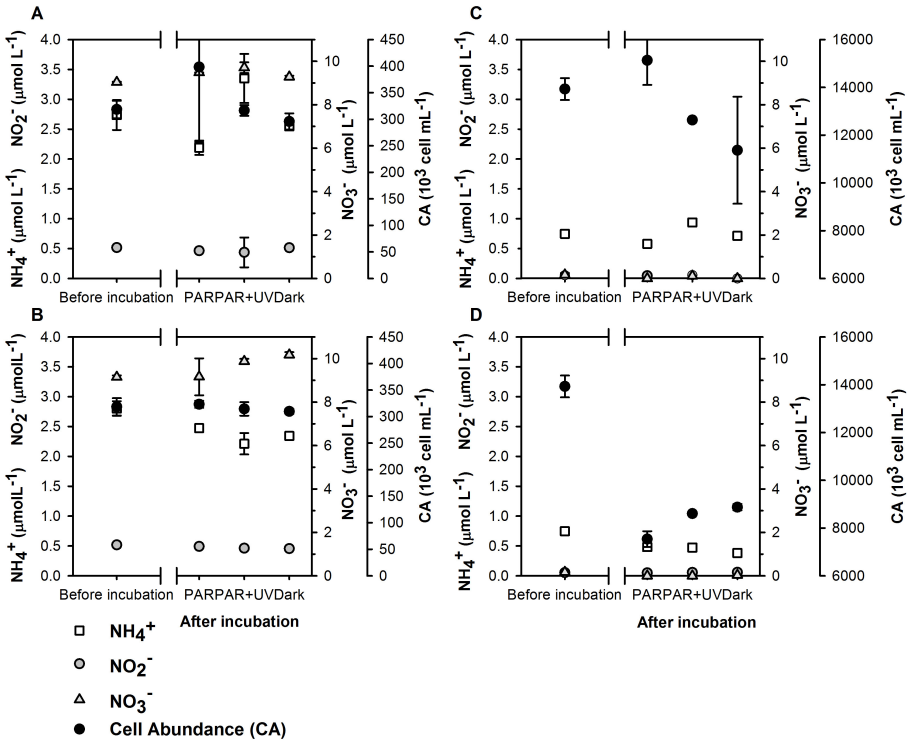

Fig. 7. Nutrient utilization experiments carried out in September 2011 and January 2012 **(A)** and **(C)** without GC-7 and **(B)** and **(D)** with GC-7 (archaeal inhibitor). Ammonium concentrations (white squares), nitrate concentrations (grey dots), nitrite concentrations (grey triangles) and bacterial abundance (black dots) are plotted as average ± standard deviation.

BGD
9, 18479–18518, 2012